と小胞体ストレスの関係を解き明かすうえで有効な手段になりうると考えられる。
BIX の虚血前の脳室内投与は用量依存的に脳保護作用を示し、梗塞体積、脳浮腫及び神経症状を有意に抑制した。梗塞巣の減少は、線条体に比べて皮質においてより強く認められた。

E．結論

マウス永久脳虚血後神経細胞死の機序の一部に小胞体ストレスの関与が示唆され、その関与は虚血中心領域よりも周辺領域において強かった。また、BiP の選択的誘導剤は新規な脳卒中治療薬のシーズとして有用である可能性が示唆された。

引用文献

1) Katayama T, Imaizumi K, Honda A, Yoneda T, Kudo T, Takeda M et al. Disturbed activation of endoplasmic reticulum stress transducers by familial Alzheimer's disease-linked presenilin 1 mutations. J Biol Chem 2001; 276: 43446-43454.

2) Paschen W, Aufenberg C, Hotop S, Mengesdorf T. Transient cerebral ischemia activates processing of xbp1 messenger RNA indicative of endoplasmic reticulum stress. J Cereb Blood Flow Metab 2003; 23: 449-461.

3) Hara H, Huang PL, Panahian N, Fishman MC, Moskowitz MA (1996) Reduced brain edema and infarction volume in mice lacking the neuronal isoform of nitric oxide synthase after transient MCA occlusion. J Cereb Blood Flow Metab 16:605-611.

4) Hara H, Friedlander RM, Gagliardini V, Ayata C, Fink K, Huang Z, Shimizu-Sasamata M, Yuan J, Moskowitz MA (1997) Inhibition of interleukin 1beta converting enzyme family proteases reduces ischemic and excitotoxic neuronal damage. Proc Natl Acad Sci USA 94:2007-2012.

G．研究発表

論文発表

1) Morimoto N., Oida Y., Shimazawa M., Miura M., Kudo T., Imaizumi K. and Hara H. Involvement of endoplasmic reticulum stress after middle cerebral artery occlusion in mice. Neuroscience, 147, 957-967, 2007.

2) Oida Y., Shimazawa M., Imaizumi K. and Hara H. Involvement of endoplasmic reticulum (ER) stress in the neuronal death induced by transient forebrain ischemia in gerbil. Neuroscience, 151, 111-119, 2008.

3) Kudo T., Kanemoto S., Hara H., Morimoto N., Morihara T., Kimura R., Tabira T., Imaizumi K and Takeda M. A molecular chaperone inducer protects neurons from ER stress. Cell Death and Differentiation, 15, 364-375, 2008.

4) Oida Y., Izuta H., Oyagi A., Shimazawa M., Kudo T., Imaizumi K. and Hara H. Induction of BiP, an ER-resident protein, prevents the neuronal death induced by transient forebrain ischemia in gerbil. Brain Res., 1208, 217-224, 2008.

2．学会発表

原英彰　虚血性神経細胞死における小胞体ストレスの関与及びその制御機構」

第 9 回日本分子脳神経外科学会　脳血管障害　研究の最前線（京都、2008、8、30-31）

研究成果の刊行に関する一覧表

雑誌

発表者氏名	論文タイトル名	発表誌名	巻号	ページ	出版年
Kudo T, Kanemoto S, Hara H, Morimoto N, Morihara T, Kimura R, Tabira T, Imaizumi K, and Takeda M.	A molecular chaperone inducer protects neurons from ER stress.	Cell Death and Differentiation	15(2)	364-375	2008
Prachasilchai W, Sonoda H, Yokota-Ikeda N, Oshikawa S, Aikawa C, Uchida K, Ito K, Kudo T, Imaizumi K, and Ikeda M.	A protective role of unfolded protein response in mouse ischemic acute kidney injury.	European Journal of Pharmacology	592(1-3)	138-145	2008
Oida Y, Shimazawa M, Imaizumi K, and Hara H.	Involvement of endoplasmic reticulum stress in the neuronal death induced by transient forebrain ischemia in gerbil.	Neuroscience	151(1)	111-119	2008
Oida Y, Izuta H, Oyagi A, Shimazawa M, Kudo T, Imaizumi K, and Hara H.	Induction of BiP, an ER-resident protein, prevents the neuronal death induced by transient forebrain ischemia in gerbil.	Brain Research	1208	217-224	2008
Yoshinaga K, Kawai K, Tanii I, Imaizumi K, and Kodama K.	Nerve fiber analysis on the so-called accessory subscapularis muscle and its morphological significance.	Anatomical Science International	83(1)	55-59	2008
Inokuchi Y, Nakajima Y, Shimazawa M, Kurita T, Kubo M, Saito A, Sajiki H, Kudo T, Aihara M, Imaizumi K, Araie M, and Hara H.	Effect of an Inducer of BiP, a Molecular Chaperon,on Endoplasmic Reticulum (ER)Stress-Induced q Retinal Cell Death.	Investigative Ophthalmology & Visual Science	50(1)	334-344	2009
Prachasilchai W, Sonoda H, Yokota-Ikeda N, Ito K, Kudo T, Imaizumi K, and Ikeda M.	The protective effect of a newly developed molecular chaperone-inducer against mouse ischemic acute kidney injury.	Journal of Pharmacological Sciences	109(2)	311-314	2009
Shinji Tagami, Masayasu Okochi, Kanta Yanagida, Akiko Ikuta, Akio Fukumori, Naohiko Matsumoto, Yoshiko Ishizuka-Katsura, Taisuke Nakayama, Naohiro Itoh, Jingwei Jiang, Kouhei Nishitomi, Kouzin Kamino, Takashi Morihara, Ryota Hashimoto, Toshihisa Tanaka, Takashi Kudo, Shigeru Chiba, and Masatoshi Takeda	Regulation of Notch Signaling by Dynamic Changes in the Precision of S3 Cleavage of Notch-1	Mol. Cell. Biol.	28	165-176	2008

Nuripa Jenishbekovna Aidaralieva, Kouzin Kamino, Ryo Kimura, Mitsuko Yamamoto, Takeshi Morihara, Hiroaki Kazui[1], Ryota Hashimoto, Toshihisa Tanaka, Takashi Kudo, Tomoyuki Kida, Jun-Ichiro Okuda, Takeshi Uema, Hidehisa Yamagata, Tetsuro Miki, Hiroyasu Akatsu, Kenji Kosaka and Masatoshi Takeda	Dynamin 2 gene is a novel susceptibility gene for late-onset Alzheimer disease in non-APOE-epsilon4 carriers.	J Hum Genet	53	296-302	2008
Masafumi Shimojo, Naruhiko Sahara, Tatsuya Mizoroki, Satoru Funamoto, Maho Morishima-Kawashima, Takashi Kudo, Masatoshi Takeda, Yasuo Ihara, Hiroshi Ichinose, and Akihiko Takashima	Enzymatic Characteristics of I213T Mutant Presenilin-1/γ-secretase in Cell Models and Knock-in Mouse Brains: FAD-linked Mutation Impairs γ-site Cleavage of APP-CTF β.	J. Biol. Chem	283(24)	16488-96	2008
Prachasilchai W, Sonoda H, Yokota-Ikeda N, Oshikawa S, Aikawa C, Uchida K, Ito K, Kudo T, Imaizumi K, & Ikeda M	A protective role of unfolded protein response in mouse ischemic acute kidney injury	European Journal of Pharmacology	592	138-145	2008
Masamitsu Shimazawa, Yuta Inokuchi, Takashi Okuno, Yoshihiro Nakajima, Gaku Sakaguchi, Akira Kato, Hidehiro Oku, Tetsuya Sugiyama, Takashi Kudo, Tsunehiko Ikeda, Masatoshi Takeda, and Hideaki Hara	Reduced retinal function in amyloid precursor protein-overexpressing transgenic mice via attenuating glutamate-N-methyl-d-aspartate receptor signaling	Journal of Neurochemistry	107	279-290	2008
Kotani Y., Nakajima Y., Hasegawa T., Satoh M., Nagase H., Shimazawa M., Yoshimura S., Iwama T. and Hara H.	Propofol exerts greater neuroprotection with disodium edentate (EDTA) than without it.	J. Cereb. Blood Flow & Metabol.,	28	354-366	2008.
Oyagi A., Oida Y., Hara H., Izuta H., Shimazawa M., Matsunaga N., Adachi T. and Hara H.	Protective effects of SUN N8075, a novel agent with antioxidant properties, in in vitro and in vivo models of Parkinson's disease.	Brain Res	1214	169-176	2008

Ito Y., Nakamura S., Tanaka H., Shimazawa M., Araie M. and Hara H.	Memantine protects against secondary neuronal degeneration in lateral geniculate nucleus and superior colliculus after retinal damage in mice.	CNS Neurosci. Ther.,	14	192-202	2008
Nonaka Y., Shimazawa M., Yoshimura S., Iwama T. and Hara H.	Combination effects of normobaric hyperoxia and edaravone on focal cerebral ischemia-induced neuronal damage in mice.	Neurosci. Lett	441	224-228	2008
Koumura A., Nonaka Y., Hyakkoku K., Oka T., Shimazawa M., Hozumi I., InuzukaT. and Hara H.	A novel calpain inhibitor, SNJ-1945, protects neuronal cells from cerebral ischemia-induced damage in mice.	Neuroscience,	157	309-318	2008
Inokuchi Y., Nakajima Y., Shimazawa M., Kurita T., Kubo M., Saito A., Sajiki H., Kudo T., Aihara M., Imaizumi K., Araie M. and Hara H	Effect of an inducer of BiP, a molecular chaperone, on endoplasmic reticulum (ER) stress-induced retinal cell death.	Invest. Ophthalmol. Vis. Sci.	50	334-344	2009
Hyakkoku K., NakajimaY., Izuta H., Shimazawa M., Yamamoto T., Shibata N. and Hara H.	Thalidomide protects against ischemic neuronal damage induced by focal cerebral ischemia in mice	Neuroscience	159	760-769	2009
Nonaka Y., Tsuruma K., Shimazawa M., Yoshimura S., Iwama T. and Hara H.	Cilostazol protects against hemorrhagic transformation in mice transient focal cerebral ischemia-induced brain damage.	Neurosci. Lett	452	156-161	2009

Cell Death and Differentiation (2008) 15, 364–375

www.nature.com/cdd

A molecular chaperone inducer protects neurons from ER stress

T Kudo*[,1,6], S Kanemoto[2,3,6], H Hara[4], N Morimoto[4], T Morihara[1], R Kimura[1], T Tabira[5], K Imaizumi*[,2] and M Takeda[1]

The endoplasmic reticulum (ER) stress response is a defense system for dealing with the accumulation of unfolded proteins in the ER lumen. Recent reports have shown that ER stress is involved in the pathology of some neurodegenerative diseases and cerebral ischemia. In a screen for compounds that induce the ER-mediated chaperone BiP (immunoglobulin heavy-chain binding protein)/GRP78 (78 kDa glucose-regulated protein), we identified BiP inducer X (BIX). BIX preferentially induced BiP with slight inductions of GRP94 (94 kDa glucose-regulated protein), calreticulin, and C/EBP homologous protein. The induction of BiP mRNA by BIX was mediated by activation of ER stress response elements upstream of the BiP gene, through the ATF6 (activating transcription factor 6) pathway. Pretreatment of neuroblastoma cells with BIX reduced cell death induced by ER stress. Intracerebroventricular pretreatment with BIX reduced the area of infarction due to focal cerebral ischemia in mice. In the penumbra of BIX-treated mice, ER stress-induced apoptosis was suppressed, leading to a reduction in the number of apoptotic cells. Considering these results together, it appears that BIX induces BiP to prevent neuronal death by ER stress, suggesting that it may be a potential therapeutic agent for cerebral diseases caused by ER stress.
Cell Death and Differentiation (2008) **15,** 364–375; doi:10.1038/sj.cdd.4402276; published online 30 November 2007

The endoplasmic reticulum (ER) is an 'assembly plant' for the manufacture of secretory and membrane proteins. However, from time to time 'inferior goods', that is, unfolded/misfolded proteins in the ER are inevitable. Under normal physiological conditions, unfolded proteins are degraded; under conditions of ER stress, however, unfolded proteins can accumulate in the ER lumen. Eukaryotes utilize the unfolded protein response (UPR) to overcome the critical status induced by ER stress.[1] The UPR consists of the following three pathways: (1) suppression of protein translation to prevent the generation of more unfolded proteins; (2) facilitation of refolding of unfolded proteins by the induction of ER chaperones; and (3) activation of ER-associated degradation (ERAD) to degrade the unfolded proteins accumulated in the ER, by the ubiquitin–proteasome pathway. If these strategies are unsuccessful, cells go into ER stress-induced apoptosis.

Recent reports show that dysregulation of the UPR is implicated in much important pathology, including some neurodegenerative diseases and cerebral ischemia. Previously, the ER transducers inositol-requiring kinase 1 (IRE1), PKR(protein kinase regulated by RNA)-like ER-associated kinase (PERK), and activating transcription factor 6 (ATF6) were reported to be downregulated in presenilin-1 mutant neurons, causing the vulnerability to ER stress seen in cases of familial Alzheimer disease (AD).[2–4] Caspase 4, the human homologue of murine caspase 12, was also reported to play a critical role in ER stress-induced neuronal cell death in AD.[5] One inherited form of Parkinson's disease is associated with the accumulation of the protein Parkin-associated endothelin receptor-like receptor in the ER of dopaminergic neurons as a result of defective ERAD by mutant Parkin, a ubiquitin protein ligase (E3).[6,7] Analysis of the polyglutamine tract associated with the spinocerebrocellular atrophy protein (spinocerebellar ataxia type 3) in Machado–Joseph disease suggests that cytoplasmic accumulation of this protein can inhibit proteasome function, thereby interfering with ERAD and eliciting ER stress-induced apoptosis.[8,9] It was also reported that cerebral ischemia activates the UPR.[10,11] These findings show that many cerebral disorders are related to an impaired UPR and ER stress-induced apoptosis.

These accumulated data concerning the involvement of ER stress in cerebral disorders encouraged us to investigate this

[1]Psychiatry, Department of Integrated Medicine, Division of Internal Medicine, Osaka University Graduate School of Medicine, Suita, Japan; [2]Division of Molecular and Cellular Biology, Department of Anatomy, Faculty of Medicine, University of Miyazaki, Miyazaki, Japan; [3]Division of Structural Cellular Biology, Nara Institute of Science and Technology (NAIST) Graduate School of Biological Sciences, Ikoma, Japan; [4]Department of Biofunctional Molecules, Gifu Pharmaceutical University, Gifu, Japan and [5]National Institute for Longevity Science, Ohbu, Japan

*Corresponding authors: T Kudo, Psychiatry, Department of Integrated Medicine, Division of Internal Medicine, Osaka University Graduate School of Medicine, D3, 2-2, Yamadaoka, Suita 565-0871, Japan. Tel: +81 6 6879 3052; Fax: +81 6 6879 3059; E-mail: kudo@psy.med.osaka-u.ac.jp or
K Imaizumi, Division of Molecular and Cellular Biology, Department of Anatomy, Faculty of Medicine, University of Miyazaki, Kihara 5200, Kiyotake, Miyazaki 889-1692, Japan. Tel: +81 985 85 1783; Fax: +81 985 85 9851; E-mail: imaizumi@med.miyazaki-u.ac.jp

[6]These authors contributed equally to this work

Keywords: endoplasmic reticulum stress; chaperone; apoptosis; cerebral ischemia; neurodegeneration

Abbreviations: AD, Alzheimer disease; ATF6, activating transcription factor 6; BiP, immunoglobulin heavy-chain binding protein; CHOP, C/EBP homologous protein; EDEM, ER degradation-enhancing α-mannosidase-like protein; eIF2α, eukaryotic translation initiation factor 2 subunit α; ERAD, ER-associated degradation; ERdj4/MDG1, ER-localized DnaJ 4/microvascular differentiation gene 1; ERSE, ER stress response element; GRP78, 78 kDa glucose-regulated protein; GRP94, 94 kDa glucose-regulated protein; HSP70, 70 kDa heat-shock protein; IRE1, inositol-requiring kinase 1; MCA, middle cerebral artery; MEF, mouse embryonic fibroblast; PERK, PKR(protein kinase regulated by RNA)-like ER-associated kinase; $p58^{IPK}$, protein kinase inhibitor of 58 kDa; Tg, thapsigargin; Tm, tunicamycin; TTC, 2,3,5-triphenyltetrazolium chloride; UPR, unfolded protein response; XBP1, X-box binding protein 1

Received 02.1.07; revised 15.10.07; accepted 18.10.07; Edited by SH Kaufmann; published online 30.11.07

field in an effort to identify therapeutic targets for the treatment of these disorders. We speculate that a therapeutic strategy that induces the UPR might prevent neuronal death induced by ER stress. According to the UPR pathway, we could try to (1) induce the expression of ER molecular chaperones; (2) block translation of proteins; or (3) artificially stimulate the degradation of misfolded proteins by the proteasome, as therapeutic approaches. Indeed, some chemical compounds that induce particular UPR pathways have been developed. For example, Boyce *et al.*[12] identified salubrinal, a selective inhibitor of cellular complexes that dephosphorylates eukaryotic translation initiation factor 2 subunit α (eIF2α), and thereby blocks translation. They concluded that salubrinal might be useful in the treatment of diseases involving ER stress.[12] Kim *et al.*[13] reported that valproate, a widely prescribed drug for epilepsy and bipolar disorder, increases the expression levels of the ER chaperones immunoglobulin heavy-chain binding protein (BiP), GRP94 (94 kDa glucose-regulated protein), protein disulfide isomerase, and calreticulin as well as the cytosolic chaperone HSP70 (70 kDa heat-shock protein). They also showed that valproate induces these chaperones without evoking the UPR, and speculated that inhibition of glycogen synthase kinase-3 by valproate might lead to the induction of chaperones.[13]

Previous reports have shown that induction of BiP, an ER molecular chaperone, prevents neuronal death induced by ER stress.[2,14–16] By contrast, inhibition of GRP78 (78 kDa glucose-regulated protein) mRNA induction increases cell death in response to calcium release from the ER, oxidative stress, hypoxia, and T-cell-mediated cytotoxicity.[17–19] Therefore, in this paper, we searched for a chemical compound that induces BiP for possible use as a neuroprotective agent against ER stress. We have identified such a chemical compound, BiP inducer X (BIX), and shown its protective effect against ER stress-induced apoptosis *in vivo* and *in vitro*, suggesting that this compound might be useful in the treatment of cerebral disorders associated with ER stress, such as cerebral ischemia.

Results

BIX preferentially induces BiP. To identify chemical compounds that induce BiP mRNA, we utilized high-throughput screening (HTS) with a BiP reporter assay system. Of the screened compounds, 1-(3,4-dihydroxyphenyl)-2-thiocyanate-ethanone (Figure 1a) showed the highest level of induction of BiP mRNA; thus, we named this compound BiP inducer X (BIX).

First, we examined whether BIX does indeed induce the expression of BiP mRNA. Northern blot analysis and real-time PCR of SK-N-SH neuroblastoma cells treated with BIX showed that BIX induces BiP mRNA in a dose-dependent manner; however, the level of BiP mRNA induced by BIX is less than that induced by thapsigargin (Tg) (Figure 1b). Additionally, treatment of cells with 50 μM BIX caused the highest induction of BiP and little toxicity to cells. Because BIX generated cytotoxicity at higher dosages, we did not use it at concentrations greater than 50 μM in further analyses. Semiquantitative RT-PCR and real-time PCR showed that the BiP signal peaked at 4 h after the addition of 5 μM BIX and remained at that level until 6 h after treatment, with a subsequent reduction in level after this point (Figure 1c). To determine whether the induction of BiP mRNA by BIX results in an increase in the level of BiP protein, we carried out immunoblot analysis. As shown in Figure 1d, the level of BiP protein was increased by 5 μM BIX in a time-dependent manner, consistent with the changes in mRNA levels.

Next, we performed semiquantitative RT-PCR analysis to investigate whether BIX affects the expression of any other ER stress response-related genes, such as GRP94, calreticulin, X-box binding protein 1 (XBP1), ER-localized DnaJ 4/microvascular differentiation gene 1 (ERdj4/MDG1), ER degradation-enhancing α-mannosidase-like protein (EDEM), protein kinase inhibitor of 58 kDa ($p58^{IPK}$), C/EBP homologous protein (CHOP), and asparagine synthetase (ASNS) (Figure 2a). According to the time-course study of BiP induction by BIX (Figure 1c), a 6 h treatment of cells with BIX was adopted into this study. XBP1 mRNA, which is spliced under ER stress induced by 1 μM Tg or 1 μg/ml tunicamycin (Tm), was not processed in cells treated with 5 μM BIX. Compared with a control sample, ERdj4/MDG1, EDEM, $p58^{IPK}$, and ASNS were scarcely induced by BIX. On the other hand, GRP94, calreticulin, and CHOP were induced by BIX, but their inductions were not as prominent as that of BiP. We also performed time-course analyses on the expressions of ER stress response-related genes by real-time PCR in SK-N-SH cells treated with 50 μM BIX as well as 5 μM BIX. A 5 μM portion of BIX induced GRP94, calreticulin, and CHOP mRNA as well as BiP. However, BiP was definitely induced from 2 to 6 h (Figure 2b). The time courses for EDEM, $p58^{IPK}$, and ASNS were not changed by treatment with 5 μM BIX (Figure 2b). A 50 μM portion of BIX also induced BiP from 4 to 6 h and transiently induced calreticulin and CHOP. Even 50 μM BIX did not induce EDEM, $p58^{IPK}$, or ASNS (Figure 2b).

Moreover, we performed immunoblot analysis of GRP94 and phosphorylated eIF2α to examine whether BIX affects other signaling pathways that participate in the ER stress response. Treatment of SK-N-SH cells with BIX caused very slight induction of GRP94 protein compared with its induction by 1 μM Tg (Figure 2c). This result was consistent with that of semiquantitative RT-PCR analysis of the GRP94 mRNA level. Treatment of cells with 1 μM Tg increased the level of phosphorylated eIF2α, but BIX did not cause its phosphorylation (Figure 2c). These results indicate that BIX invokes little ER stress, but almost preferentially induces BiP.

The induction of BiP by BIX is mediated by activation of ERSEs through the ATF6 pathway. To investigate the mechanism by which BiP is induced by BIX, we performed reporter assays using 132 bp BiP-pGL3 reporter plasmids as described in the Materials and Methods section. A BiP (132)-pGL3 plasmid (Figure 3a) was transfected into SK-N-SH cells and the cells were treated with 5 μM BIX, 300 nM Tg, or 0.5 μg/ml Tm for either 6 or 16 h. The reporter activities in transfectants were elevated in response to stimulation with Tg or Tm, and maintained at a long-lasting high level (Figure 3b). By contrast, reporter activities in cells treated with BIX were transiently induced at 6 h after stimulation and then downregulated to basal levels by 16 h (Figure 3b). This

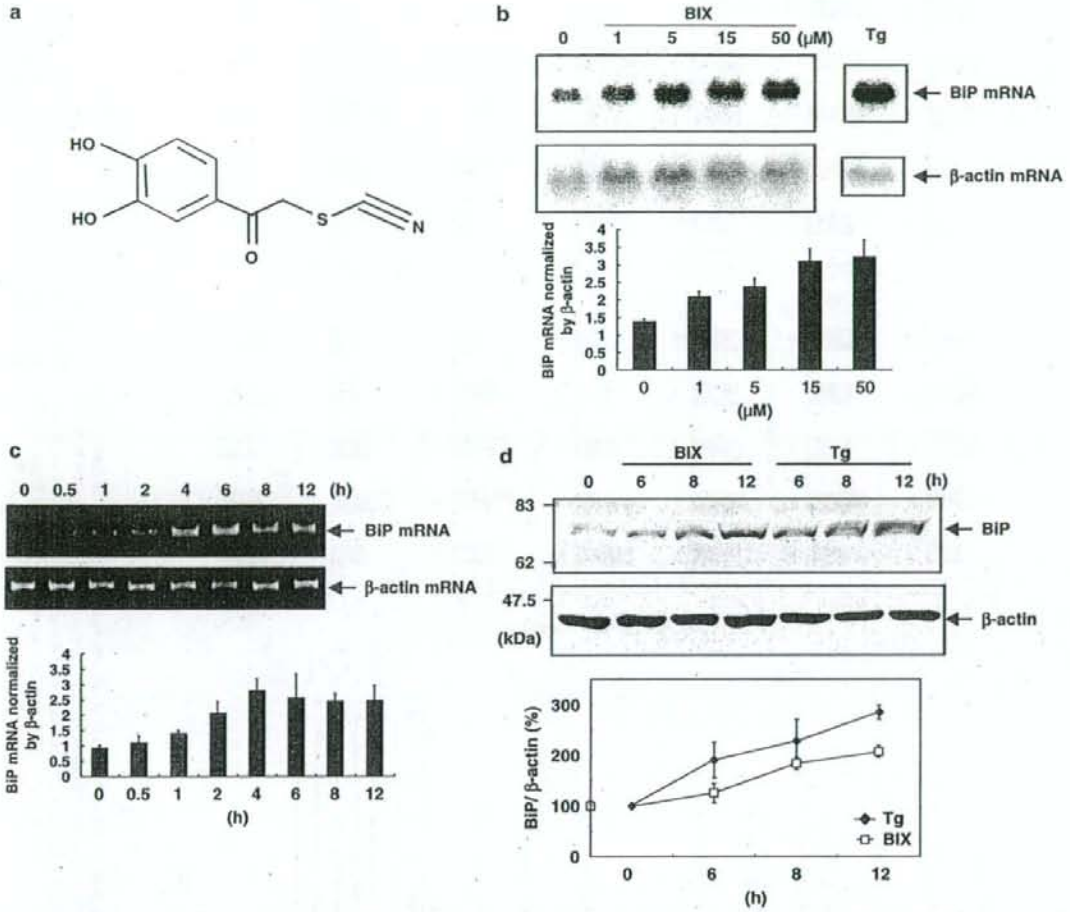

Figure 1 BIX induces BiP. (**a**) The structure of BIX (1-(3,4-dihydroxyphenyl)-2-thiocyanate-ethanone). (**b**) Dose-dependent induction of BiP mRNA in SK-N-SH cells after 6 h of treatment with BIX is shown by northern blot (upper panel) and real-time PCR (lower panel); values are means ± S.D. from three independent experiments. The induction of BiP mRNA by Tg is shown as a positive control. β-Actin mRNA is shown as an internal control. (**c**) The time course of BiP mRNA induction in cells treated with BIX is shown by semiquantitative RT-PCR (upper panel) and real-time PCR (lower panel); values are means ± S.D. from three independent experiments. The level of BiP mRNA peaked in 4 h and kept until 6 h after treatment with BIX at 5 μM, with a subsequent reduction after this point. (**d**) A time-dependent induction of BiP protein in SK-N-SH cells treated with 5 μM BIX or 1 μM Tg is detected by immunoblot and quantified by densitometry. Values are means ± S.D. from three independent experiments

finding supports the results shown in Figure 1c and suggests that the effects of BIX on BiP induction are transient and that BiP mRNA reverts to basal levels. Therefore, induction of BiP by BIX might be caused by a mechanism different to that used by ER stressors such as Tg and Tm, and the BIX-responsive element(s) might be included in the 132 bp BiP promoter region. Within this 132 bp region, there are three ER stress response elements (ERSEs) (Figure 3a). Subsequently, we carried out the reporter assay using an ERSE mut (132)-pGL3 plasmid (Figure 3a) to confirm whether or not these ERSEs are involved in the induction of BiP by BIX. BiP (132)-pGL3 or ERSE mut (132)-pGL3 was transfected into SK-N-SH cells, and the cells were treated with 5 μM BIX for 6 h. The reporter activities in cells transfected with BiP (132)-pGL3 were increased ~4-fold by BIX. On the other hand, induction of reporter activity was not observed in cells transfected with ERSE mut (132)-pGL3 (Figure 3c). This result suggests that ERSEs are involved in the induction of BiP by BIX.

Next, to examine whether three major transducers of the ER stress response, namely PERK, IRE1, and ATF6, affect the induction of BiP by BIX, we analyzed the expression of BiP in knockout/knockdown mouse embryonic fibroblasts (MEFs) lacking each transducer (Figure 3d). In PERK-deficient MEFs and IRE1α/β double-knockout MEFs, BiP mRNA was induced by BIX to a similar level to that seen in wild-type cells

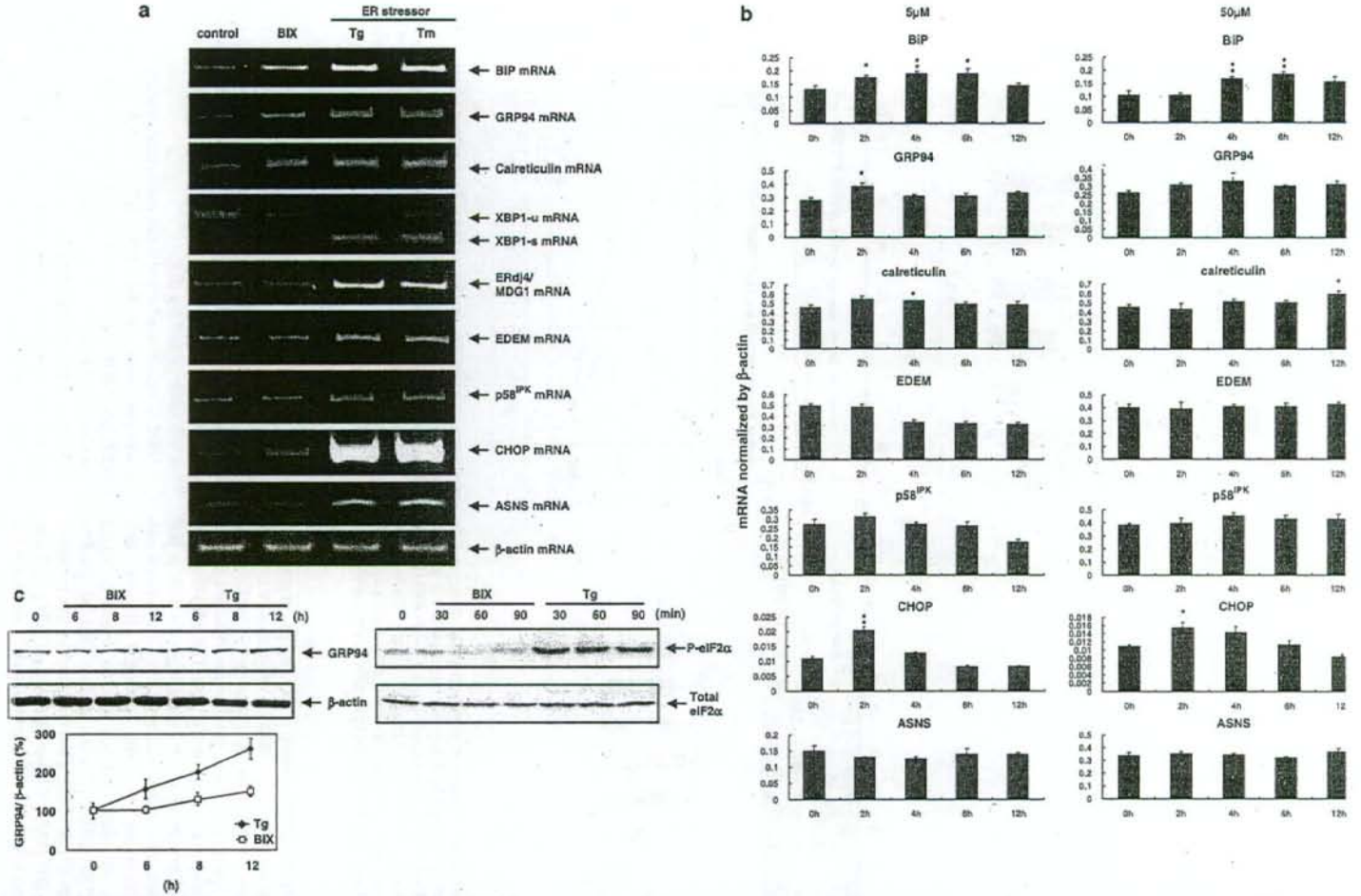

Figure 2 BIX preferentially induces BiP. (a) Semiquantitative RT-PCR analysis shows that a 6 h treatment of cells with 5 μM BIX induces BiP mRNA but not spliced XBP1 (XBP1-s), ERdj4/MDG1, EDEM, p58^{IPK}, and ASNS mRNAs, which are induced by 1 μM Tg or 1 μg/ml Tm. GRP94, calreticulin, CHOP are slightly induced by BIX. (b) Time-course analyses by real-time PCR show that 5 μM BIX significantly induces BiP from 2 to 6 h after BIX administration and transiently induces GRP94, calreticulin, and CHOP. The mRNAs of EDEM, p58^{IPK}, and ASNS are not changed from 2 to 12 h. A 50 μM portion of BIX also induces BiP from 4 to 6 h and transiently induces calreticulin and CHOP. Even 50 μM BIX does not induce EDEM, p58^{IPK}, and ASNS. Values are means ± S.E. from 3–4 independent experiments. Significant differences are based on the values at 0 h, $^{*}P<0.05$, $^{**}P<0.01$. (c) Immunoblot analysis with quantification shows that 5 μM BIX causes very slight induction of GRP94 protein but does not induce the phosphorylation of eIF2α at any time point, compared with 1 μM Tg. Values are means ± S.D. from three independent experiments

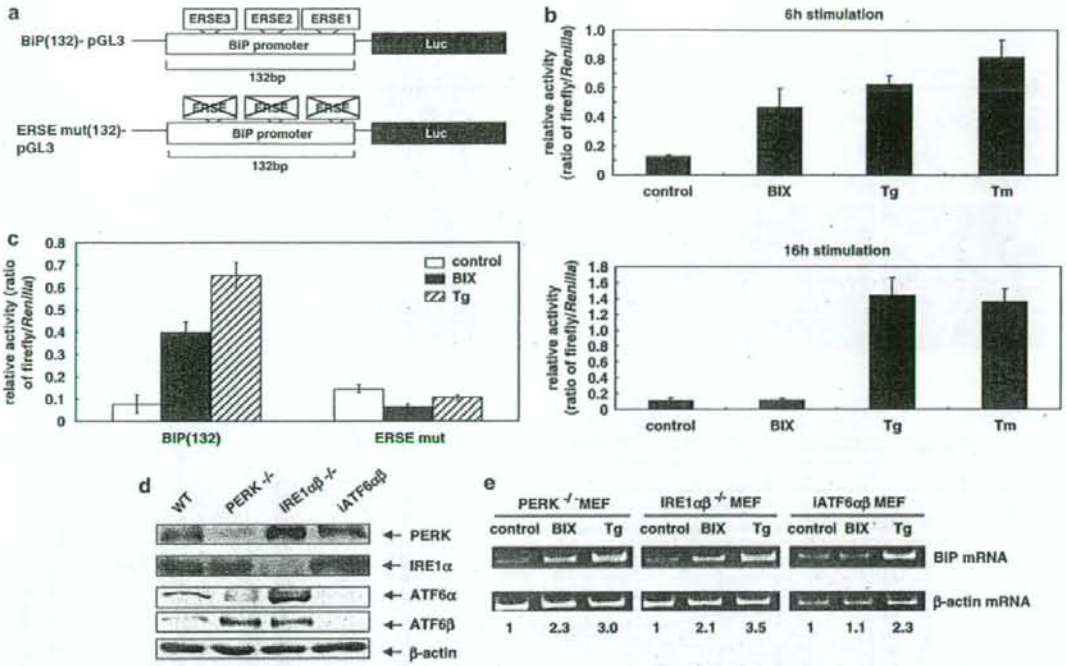

Figure 3 The induction of BiP by BIX is mediated by ERSE and the ATF6 pathway. (**a**) Schematic representation of the BiP promoter cloned into the pGL3 plasmid (BiP (132)-pGL3) and the ERSE mutant BiP promoter cloned into the pGL3 plasmid (ERSE mut (132)-pGL3). (**b**) The luciferase activities driven by the BiP promoter are normalized against *Renilla* luciferase activities. The induction of luciferase activity in BiP (132)-pGL3-transfected cells that are treated with 5 μM BIX increased at 6 h after BIX treatment and reversed to basal levels by 16 h. Induction of luciferase activity in 300 nM Tg- or 0.5 μg/ml Tm-treated cells is sustained until 16 h after BIX treatment. Values are means ± S.D. from five independent experiments. (**c**) The relative reporter activity in cells transfected with BiP (132)-pGL3 (ratio of firefly/*Renilla*) at 6 h after treatment in cells treated with BIX (5 μM) are increased ~4-fold, whereas that in cells transfected with ERSE mut (132)-pGL3 are not increased. Values are means ± S.D. from five independent experiments. Tg (300 nM) also increases reporter activity in cells transfected with BiP (132)-pGL3, but not in cells transfected with mut (132)-pGL3. (**d**) Immunoblot analyses of PERK$^{-/-}$ MEFs, IRE1$\alpha\beta^{-/-}$ MEFs, and iATF6$\alpha\beta$ (knockdown) MEFs with anti-PERK, anti-IRE1 and anti-ATF6α/β antibodies prove the deficiency of those genes. (**e**) Semiquantitative RT-PCR analysis shows that BiP mRNA is induced at 6 h after treatment with BIX (50 μM) in PERK$^{-/-}$ MEFs and IRE1$\alpha\beta^{-/-}$ MEFs, but not in iATF6$\alpha\beta$ (knockdown) MEFs. Tg induces BiP mRNA in all three MEFs. Numeric values below the panels indicate the induction ratio of BiP mRNA adjusted to the level of β-actin mRNA with reference to non-treated control sample as one

(Figure 3e). These results indicate that the induction of BiP by BIX is not mediated via the PERK or IRE1 pathways. The data showing that eIF2α is not phosphorylated by BIX (Figure 2c), and that XBP1 is not processed by BIX (Figure 2a), support this conclusion. By contrast, BiP was not induced by BIX in ATF6$\alpha\beta$ double-knockdown MEFs (Figure 3e), suggesting that BIX treatment mediates the induction of BiP via the ATF6 pathway. These results were also obtained by northern blot analysis (data not shown). The data showing that BIX induced GRP94, calreticulin, and CHOP, and that ERdj4/MDG1, EDEM, p58^{IPK} and ASNS were not induced by BIX (Figure 2a, b), also suggested that the effect of BIX is mediated by the ATF6 pathway. This is because the inductions of GRP94, calreticulin, and CHOP are known to be dependent on the activation of ATF6; inductions of ERdj4/MDG1, EDEM, p58^{IPK} are known to be mediated by IRE1 and that of ASNS by PERK. Next, we tried to detect the cleavage of ATF6 in cells treated with BIX, but we have not yet detected cleaved N-terminal fragments of endogenous ATF6 using the antibody described in this study (data not shown).

BIX protects SK-N-SH cells from ER stress-induced apoptosis. BiP functions as a cytoprotective protein in stressed cells.[14–16] As BIX activates BiP expression, BIX might protect cells from ER stress. To investigate whether BIX has the ability to prevent apoptosis induced by ER stress, SK-N-SH cells were pretreated for 12 h with 0 or 5 μM BIX, which was then replaced with fresh medium containing 0.5 μg/ml Tm. Phase-contrast images (Figure 4a–d) and fluorescence micrographs (Figure 4e–h) of Hoechst staining show that apoptotic cell death was observed within 36 h of Tm treatment (Figure 4d, h), and that the number of dead cells had increased significantly (Figure 4i). By contrast, cell death was significantly inhibited by pretreatment with BIX (Figure 4c, g, i). We also found that treatment of cells with BIX only for 36 h caused no changes in cells (Figure 4b, f). Next, we looked at the activation of caspases 4 and 3/7 after ER stress. Caspase 4 was reported to be activated in response to ER stress in human cells.[5] Immunoblot analysis showed that pretreatment of cells with BIX attenuated the cleavage of caspase 4 (Figure 4j). Moreover, we analyzed

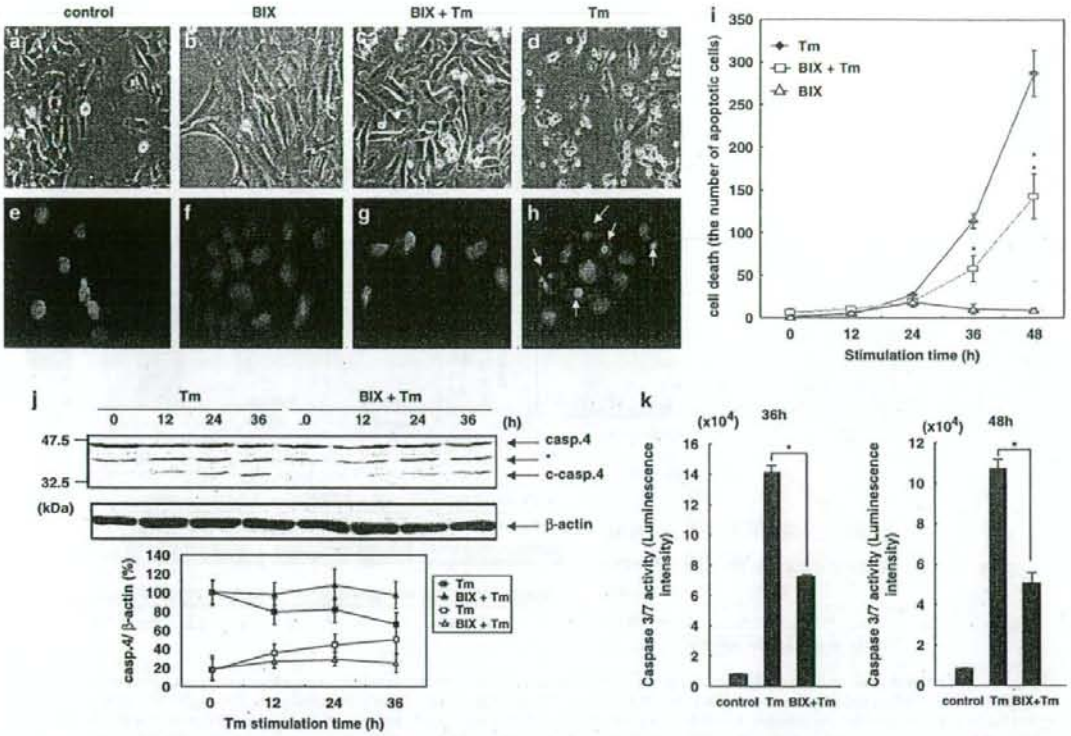

Figure 4 BIX protects SK-N-SH cells from ER stress-induced apoptosis. SK-N-SH cells are pretreated with vehicle (control: **a**, **e**; Tm: **d**, **h**) or with 5 μM BIX (BIX: **b**, **f**; BIX + Tm: **c**, **g**) for 12 h, and then the whole medium is replaced with fresh medium (control, BIX) or medium supplemented with 0.5 μg/ml Tm (BIX + Tm, Tm). Phase-contrast images (**a**–**d**) and fluorescence micrographs of Hoechst staining (**e**–**h**) at 36 h after Tm stimulation show that pretreatment of cells with BIX reduces the number of Tm-induced apoptotic cells. Arrows show apoptotic cells (**h**). (**i**) The number of dead cells (apoptotic cells) after Tm treatment increases from 0 to 48 h. Pretreatment of cells with BIX significantly reduces the amount of cell death compared with cells treated with Tm only (*$P<0.05$, **$P<0.01$). BIX alone does not cause remarkable cell death. A total of 500 cells are counted at each time point. Values are means ± S.D. from five independent experiments. (**j**) Immunoblot of caspase 4 shows that Tm causes cleavage of caspase 4 (c-Casp.4) in a time-dependent manner and that pretreatment of cells with BIX attenuates this cleavage with no change in the level of β-actin. Asterisk indicates nonspecific bands. The lower panel shows quantitative analyses of full-length and cleaved caspase 4. Filled square and triangle indicate full-length caspase 4; open square and triangle indicate cleaved caspase 4. Values are means ± S.D. from three independent experiments. (**k**) The caspases 3 and 7 activities in Tm-treated cells are increased. BIX reduces this caspase activity to almost half value of the Tm-treated levels. Values are means ± S.D. from three independent experiments; *$P<0.01$

the activities of caspases 3 and 7. The activities of caspases 3 and 7 in Tm-treated cells were extremely high. By contrast, BIX reduced the activities of caspases 3 and 7 to half of those in cells treated with Tm only (Figure 4k). Taken together, these findings suggest that pretreatment of cells with BIX inhibits cell death induced by ER stress involving inhibited activation of caspases 3/7 and 4.

BIX administration reduces the insults due to cerebral infarction. Because it has been shown that cerebral ischemia causes ER stress,[20] we performed occlusions of the middle cerebral arteries (MCAs) of mice to confirm whether the protective effects of BIX *in vitro* can be utilized *in vivo*. Immunoblot analysis of extracts from the cerebral hemisphere showed that 20 μg (2 μl) of BIX (administered intracerebroventricularly) significantly increased the level of BiP protein 24 h after administration, confirming that administration of BIX induces BiP protein *in vivo* (Figure 5a). Real-time PCR analysis of the expression of ER stress response-related genes showed that 20 μg BIX significantly induced BiP at 6 h after administration (Figure 5b). The levels of GRP94, calreticulin, and CHOP mRNA also increased; however, those of EDEM, $p58^{IPK}$, and ASNS did not change (Figure 5b), consistent with the results of *in vitro* study (Figure 2b). Animals treated with BIX showed no behavioral changes, except for the neurological deficits induced by ischemia. Neurological evaluation at 24 h after MCA occlusion showed that most of the vehicle-administered (control) mice presented with moderate symptoms; for example, circling to the contralateral side (Figure 5c). By contrast, most BIX-administered (5 or 20 μg) mice presented with milder symptoms; for example, extending the right forepaw (Figure 5c).

Twenty-four hours after occlusion, 2,3,5-triphenyltetrazolium chloride (TTC) staining showed that the mice had developed infarcts affecting the ipsilateral cortex and striatum

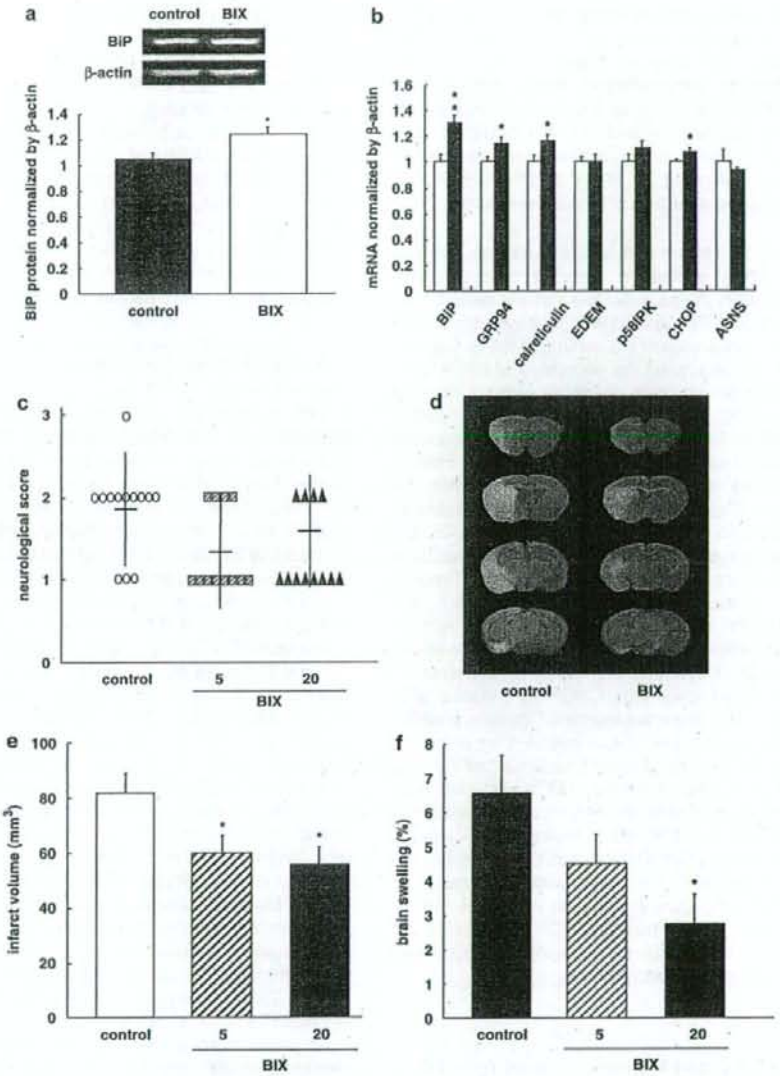

Figure 5 BIX administration reduces the extent of cerebral infarction after MCA occlusion. (a) It is confirmed that intracerebroventricular administration of BIX raises the level of BiP protein in mouse brains. Immunoblot analysis of BiP and β-actin protein in BIX-administered (20 μg/2 μl) brains shows that the level of BiP protein is significantly increased at 24 h after BIX administration compared with vehicle-treated brains. The inset is the representative immunoblot detected by luminescence of ECL. Densitometric scanning of BiP bands normalized to β-actin was performed. Data are represented as means ± S.E. from four independent experiments; $^{*}P<0.05$. (b) The real-time PCR shows that the level of BiP (in arbitrary units) in the BIX-administered (20 μg/2 μl) hemisphere is increased significantly at 6 h after administration. The levels of GRP94, calreticulin, and CHOP mRNA are increased by BIX; the levels of EDEM, p58^{IPK}, and ASNS do not change. The black bar is the BIX-administered (20 μg/2 μl) hemisphere; the white bar is the vehicle-administered hemisphere. Values are means ± S.E. from 3–4 independent experiments; $^{*}P<0.05$, $^{**}P<0.01$. (c) Neurological deficits at 24 h after occlusion of the MCA are scored using the following scale: 0 = no observable neurological deficits (normal); 1 = failure to extend the right forepaw (mild); 2 = circling to the contralateral side (moderate); 3 = loss of walking or righting reflex (severe). BIX administration (5 or 20 μg) improves neurological deficits induced by MCA occlusion. Values are means (horizontal bold bar) ± S.D. (d) Representative images of TTC staining at 24 h after MCA occlusion. Note that the infarct area (white or pink) in BIX-administered brains is smaller than that in brains treated with vehicle. (e) Quantitative analysis of infarct volumes measured by TTC staining. Values are means ± S.E. from 12 or 13 independent experiments; $^{*}P<0.05$. (f) BIX administration (5 or 20 μg) reduces brain swelling induced by MCA occlusion. Values are means ± S.E. from 12 or 13 independent experiments; $^{*}P<0.05$

(Figure 5d). The core of infarction was observed as a white area and the penumbra was pink. The infarction area (core + penumbra) observed in BIX-treated brains was smaller than that in vehicle-treated brains (Figure 5d). Quantitation of TTC staining showed that administration of 5 or 20 μg of BIX significantly reduced the infarction area (Figure 5e). Furthermore, measurement of brain swelling also showed that administration of 20 μg of BIX significantly reduced brain swelling after 24 h of ischemia (Figure 5f).

BIX administration reduces apoptosis induced in the penumbra by MCA occlusion. Detailed observation of TTC-stained ischemic brains indicated that the reduction in the area of infarction in BIX-treated brains was predominantly due to a reduction in the area of the penumbra rather than the core. Therefore, we examined the penumbra of BIX-treated brain for evidence of apoptosis. Terminal deoxynucleotidyl transferase-mediated dUTP–biotin nick end labeling (TUNEL) staining of ischemic brains without BIX treatment revealed an increased number of TUNEL-positive cells in the ipsilateral core and penumbra compared with the contralateral side (Figure 6a). By contrast, the number of TUNEL-positive cells was significantly reduced in the ipsilateral penumbra of BIX-treated brains compared with that of vehicle-treated brains (Figure 6a, b). Immunohistochemistry for caspase 3 in the penumbrae of BIX- and vehicle-treated brains showed that BIX reduced the number of apoptotic cells at 24 h after MCA occlusion (Figure 6c, d). CHOP plays a role in apoptotic cell death by ER stress.[21] Moreover, it is well-known that CHOP is induced after ischemic insults.[22] Therefore, we examined the effects of BIX treatment on the induction of CHOP mRNA after ischemia. *In situ* hybridization analysis showed that CHOP mRNA was significantly induced in the penumbra of MCA-occluded mice, whereas pretreatment of mice with BIX resulted in a marked reduction in the level of CHOP mRNA expression (Figure 6e, f). Although BIX induced CHOP (Figure 5b), the extent of this induction was very weak compared with the expression induced by ischemia (Figure 6e, f). The results of TUNEL staining and *in situ* hybridization for CHOP indicate that BIX suppresses the ER stress-mediated apoptotic cell death induced in the penumbra after ischemia.

Discussion

If a BiP inducer is just an ER stressor such as Tg or Tm, its application as a therapeutic strategy is unlikely to be realized because it may activate several pathways of the UPR, including ER stress-induced apoptotic pathways. The present studies in knockout or knockdown MEFs deficient in ER stress sensors showed that the ATF6 pathway is necessary for BIX to induce BiP. This is consistent with the evidence that BIX preferentially induced BiP with slight inductions of GRP94, calreticulin, and CHOP mediated by the ATF6 pathway, and that BIX does not affect the pathway downstream of IRE1 or the translational control branch downstream of PERK. Moreover, for the apoptotic branches of ER stress, the transient induction of CHOP by BIX was very weak compared with the severe induction observed in ER stress, and caspase 4 was not activated by BIX. The differences among inductions between BiP and the other genes of the ATF6 pathway by BIX suggested that elements other than ERSEs may be involved in the induction of BiP by BIX.

The present data from *in vitro* studies showed that BIX suppresses the cleavage of caspase 4, a member of one of the apoptotic pathways mediated by ER stress. Because it was reported that PERK is activated after cerebral ischemia[10] and that XBP1 mRNA splicing is detected after transient cerebral ischemia,[11] it would appear that cerebral ischemia causes ER stress. Thus, to examine the antiapoptotic effect of BIX *in vivo*, we used MCA-occluded mice. Intracerebroventricular pretreatment of mice with BIX reduced the area of infarction in the brain, especially the area of the penumbra. BIX pretreatment also reduced the severity of neurological deficits caused by focal cerebral ischemia. In the penumbrae of BIX-treated brains, the induction of CHOP, an apoptotic molecule induced by ER stress, was suppressed, suggesting that BIX reduces cell death by preventing ER stress-induced apoptosis. As the infarct volumes, brain swelling, and neurological scores following 5 and 20 μg treatments were similar, 5 μg of BIX might be sufficient to protect against ischemia. This is the first report demonstrating the *in vivo* success of a therapeutic manipulation to inhibit apoptosis mediated by ER stress, indicting that BIX might be a potential therapeutic for neuroprotection after cerebral infarction.

The induction of BiP by BIX was transient, peaking at 4 h after treatment, but the levels of BiP protein continued to increase until 12 h. The reporter assay using the 132 bp BiP-pGL3 plasmid also showed that the effect of BIX on the induction of BiP was transient and weaker than the effect of ER stressors, such as Tg or Tm. Even a high dosage of BIX (50 μM) did not induce genes mediated by non-ATF6 pathways. These results imply that the mechanism of BiP induction utilized by BIX may be different from those used by these ER stressors. It was reported that the activation of transducers of ER stress is caused by dissociation of BiP from their luminal domains.[23] It may be assumed that artificial induction of BiP disturbs the activation of transducers of ER stress, because abundant BiP remains bound to these transducers preventing their activation. However, the effect of BIX peaked at 4 h and remained at that level until 6 h after treatment; after this point, there was a subsequent reduction in level. Therefore, the production of BiP induced by BIX may not disturb this dissociation.

An earlier study showed that a selective inhibitor of eIF2α dephosphorylation protects cells from ER stress[12] and that the development of novel chemical compounds for diseases related to ER stress is underway. It is possible that BIX, which has effects *in vivo*, could have therapeutic applications in the treatment of diseases involving ER stress. We propose that BiP activators, such as BIX, will be effective agents against ER stress. However, further studies will be required to investigate the pharmacology of BIX, including its possible side effects, before BiP activators can be used in clinical practice.

Materials and Methods

Cell culture. SK-N-SH neuroblastoma cells were grown in α-modified Eagle's medium supplemented with 10% fetal bovine serum. MEFs derived from IRE1$^{-/-}$ embryos or PERK$^{-/-}$ embryos were cultured in Dulbecco's modified Eagle's

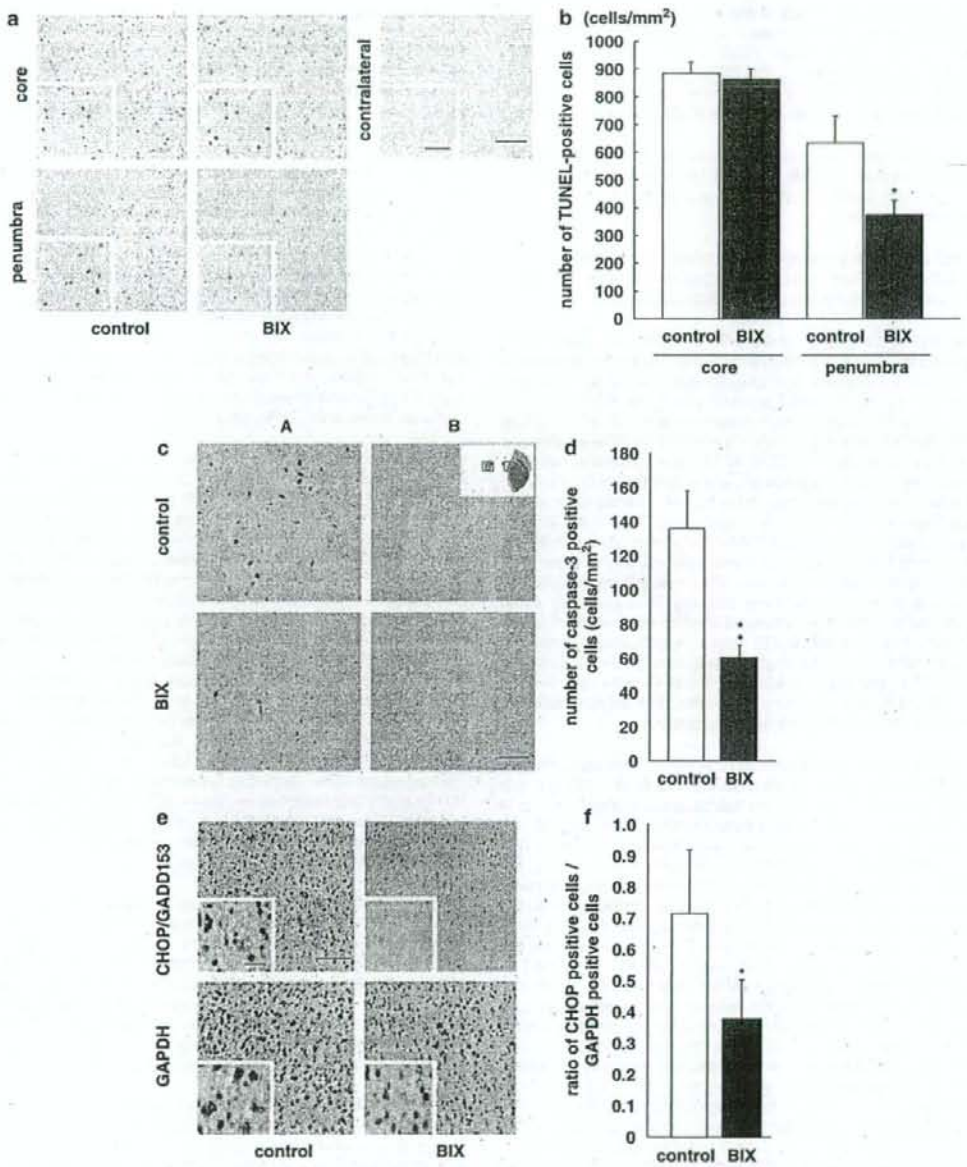

Figure 6 A 20 μg portion of BIX administration reduces ER stress-induced apoptosis induced in the penumbra by MCA occlusion. (a) Representative images of TUNEL staining in the core, penumbra, or contralateral side to the infarction at 24 h. Insets are higher magnification images. BIX administration reduces the number of TUNEL-positive cells induced in the penumbra by MCA occlusion. Scale bar for higher magnification panels, 10 μm; lower magnification panels, 100 μm. (b) Cell-counting analysis shows that BIX significantly reduced the number of TUNEL-positive cells in the penumbra. Values are means ± S.D. from 9 or 10 independent experiments; $^{*}P<0.05$. (c) Representative image showing immunohistochemical staining for caspase 3 in the penumbra area (**A**) and contralateral area (**B**) in a BIX-treated mouse and vehicle-treated mouse at 24 h after treatment. Scale bar, 50 μm. (d) Quantitative analysis of caspase 3-positive cells. Values shown are the number of caspase 3-positive cells/mm^2. Values are means ± S.D. from five independent experiments; $^{**}P<0.01$. (e) Representative images of *in situ* hybridization for CHOP, an apoptotic molecule induced in penumbra by ER stress at 24 h. Insets are higher magnification images. Scale bar for higher magnification panels, 10 μm; lower magnification panels, 100 μm. (f) Quantitative analysis of CHOP-positive cells. Values shown are the ratios of CHOP-/GAPDH-positive cells. Values are means ± S.D. from five independent experiments; $^{*}P<0.05$

medium supplemented with 10% fetal bovine serum. MEFs in which both ATF6α and ATF6β (iATF6αβMEF) had been knocked down were also maintained in the Dulbecco's modified Eagle's medium. $PERK^{-/-}$ MEFs, $IRE1^{-/-}$ MEFs, and iATF6αβMEFs were kindly provided by Drs. David Ron (New York University, NY, USA), Dr. Fumihiko Urano (University of Massachusetts Medical School, MA, USA), and Laurie H Glimcher (Harvard School of Public Health, MA, USA), respectively.

Reagents. Cells were treated with Tm or Tg to induce ER stress conditions. Tm was purchased from Sigma (St. Louis, MO, USA). Tg was purchased from Alomone Labs Ltd (Jerusalem, Israel). Hoechst staining was performed according to the manufacturer's instructions.

Plasmids. A pGL3-BiP promoter (132)-Luc reporter plasmid (BiP (132)-pGL3) and an ERSE mutant BiP promoter-Luc reporter plasmid (ERSE mut (132)-pGL3) were provided by Dr. K Mori (Kyoto University, Kyoto, Japan).

Transfection and reporter assays. SK-N-SH cells were grown to 80% confluence and then transfected using Lipofectamine 2000 reagent, according to the manufacturer's instructions (Invitrogen, Carlsbad, CA, USA). Cells were transfected with a reporter plasmid (0.2 μg) carrying the firefly luciferase gene under the control of the BiP promoter, and a reference plasmid pRL-SV40 (0.02 μg) carrying the *Renilla* luciferase gene under the control of the SV40 enhancer and promoter (Promega, Madison, WI, USA). At 12 h after transfection, cells were treated with library compounds to screen for compounds that induce BiP. Firefly and *Renilla* luciferase activities were measured in 10 μl of cell lysate using a Dual-Luciferase Reporter Assay System (Promega) and a luminometer (Berthold Technologies, Bad Wildbad, Germany). Relative luciferase activity was defined as the ratio of firefly luciferase activity to *Renilla* luciferase activity. Values were averaged from quadruplicate determinations. Using these BiP reporter cells, HTS was performed on a compound library consisting of approximately 10 000 compounds. The molecules were synthesized based on the structures of 10 lead compounds that had high activity in HTS. Among the synthesized molecules, we chose a small molecule that had the highest activity, naming it BIX. To confirm the induction of BiP by this compound, 5 μM BIX, 300 nM Tg or 0.5 μg/ml Tm were added to cell and the luciferase assay was performed as described; luciferase activities were measured in three independent experiments.

RNA isolation and semiquantitative RT-PCR analysis. SK-N-SH cells or MEFs were washed with phosphate-buffered saline (PBS) and then collected by centrifugation. Total RNA was isolated from cells using an RNeasy kit (Qiagen, Tokyo, Japan) according to the manufacturer's protocol. Total RNA was isolated from frozen brains using the acid guanidine–phenol–chloroform RNA extraction method provided as ISOGEN (Nippon Gene, Toyama, Japan), and purified using an RNeasy Mini kit (Qiagen). RNA concentrations were determined spectrophotometrically at 260 nm. First-strand cDNA was synthesized in a 20-μl reaction volume using a random primer (Takara, Shiga, Japan) and Moloney murine leukemia virus reverse transcriptase (Invitrogen). PCR was performed in a total volume of 30 μl containing 0.8 μM of each primer, 0.2 mM dNTPs, 3 U *Taq* DNA polymerase (Promega), 2.5 mM $MgCl_2$, and 1 × PCR buffer. The amplification conditions for semiquantitative RT-PCR analysis were as follows: an initial denaturation step of 95°C for 5 min, 22 cycles of 95°C for 1 min, 55°C for 1 min, and 72°C for 1 min, and a final extension step of 72°C for 7 min. The numbers of amplification cycles for detection of BiP and β-actin were 18 and 15, respectively. The primers used for amplification were as follows: BiP: 5′-GTTTGCTGAGG AAGACAAAAAGCTC-3′ and 5′-CACTTCCATAGAGTTTGCTGATAATTG-3′; XBP1: 5′-CAGCGCTTGGGGATGGATGC-3′ and 5′-CCATGGGGAGATGTTCTG GA-3′; CHOP: 5′-GGAGCTGGAAGCCTGGTATGAGG-3′ and 5′-TCCCTGGTCA GGCGCTCGATTTCC-3′; GRP94: 5′- CTCACCATTTGGATCCTGTGTG-3′ and 5′-CACATGACAAGATTTTACATCAAGA-3′; calreticulin: 5′-GCCAAGGACGAGCT GTAGAGAG-3′ and 5′-GGTGAGGGCTGAAGGAGAATC-3′; ERdj4/MDG1: 5′-TCTAGAATGGCTACTCCCCAGTCAATTTTC-3′ and 5′-TCTAGACTACTGTCCT GAACAGTCAGTG-3′; EDEM: 5′-TGGGTTGGAAAGCAGAGTGGC-3′ and 5′-TCCATTCCTACATGGAGGTAG-3′; $p58^{IPK}$ 5′-GAGGTTTGTGTTTGGGATGCAG-3′ and 5′-GCTCTTCAGCTGACTCAATCAG-3′; ASNS: 5′-AGGTTGATGATGCAATG ATGG-3′ and 5′-TCCCCTATCTACCCACAGTCC-3′; β-actin: 5′-TCCTCCCTGGA GAAGAGCTAC-3′ and 5′-TCCTGCTTGCTGATCCACAT-3′. PCR products were resolved by electrophoresis through 4.8% (w/v) polyacrylamide gels. The density of each band was quantified using the Scion Image Program (Scion Corporation, Frederick, MD, USA).

Northern blot analysis. Total RNA (10 μg/lane) was resolved by electrophoresis through 1.0% agarose/formaldehyde gels and transferred onto Immobilon-NY + membranes (Millipore, Bedford, MA, USA). Filters were hybridized with ^{32}P-labeled cDNA probes generated from the BiP cDNA by the Random Primer DNA labeling kit (Takara). After washing in 2 × SSC/0.1% SDS and 0.1 × SSC/0.1% SDS, filters were exposed onto IP plates (Fuji Film, Tokyo, Japan) and analyzed using a BAS1800 system (Fuji Film).

Real-time PCR. TaqMan real-time PCR was performed as described previously.[74] Single-stranded cDNA was synthesized from total RNA using a High-Capacity cDNA Archive Kit (Applied Biosystems, Foster City, CA, USA). Quantitative real-time PCR was performed using an ABI PRISM® 7900HT Sequence Detection System (Applied Biosystems) with a TaqMan Universal PCR Master Mix (Applied Biosystems) according to the manufacturer's protocol. The expressions of mRNAs were measured by real-time PCR using the Applied Biosystems Assays-on-Demand™ Gene Expression Product. The thermal cycler conditions were as follows: 2 min at 50°C and then 10 min at 95°C, followed by two-step PCR for 50 cycles consisting of 95°C for 15 s followed by 60°C for 1 min. For each PCR, we checked the slope value, R^2 value, and linear range of a standard curve of serial dilutions. All reactions were performed in duplicate. The results are expressed relative to the β-actin, internal control.

Immunoblot analysis. Cells were washed with PBS, harvested and lysed in Nonidet P-40 lysis buffer (1% Nonidet P-40, 20 mM HEPES (pH 7.6), 100 mM NaCl, 3 mM $MgCl_2$, 5 mM dithiothreitol, and 0.1% protease inhibitor cocktail (Sigma)). Lysates were then sonicated on ice three times for 5 s and centrifuged at 15 000 r.p.m. for 5 min. Supernatants were retained and boiled for 5 min in SDS sample buffer. Equal amounts of protein were subjected to 10–15% SDS-PAGE, transferred to PVDF membranes, and immunoblotted with each primary antibody. Membranes were washed with TBS/Tween-20, and then incubated with an alkaline phosphatase-conjugated secondary antibody (Sigma). The corresponding bands were detected using ECL Plus Western Blotting Detection System (GE Healthcare UK Ltd, Buckinghamshire, England). The density of each band was quantified using the Scion Image Program (Scion Corporation). As primary antibodies, anti-PERK antibody was provided by Dr. David Ron (New York University) and anti-IRE1α antibody was provided by Dr. Fumihiko Urano (University of Massachusetts Medical School). Anti-KDEL (Stressgen, Victoria, BC, Canada), anti-total eIF2α (Cell signaling Technology, Beverly, MA, USA), anti-eIF2α (phosphospecific) (Stressgen), anti-ATF6α (Santa Cruz Biotechnology, Santa Cruz, CA, USA), anti-ATF6β (Santa Cruz Biotechnology), anti-TX (MBL Co. Ltd, Nagoya, Japan), and anti-actin (Chemicon, Temecula, CA, USA) antibodies were purchased commercially. Anti-KDEL antibody detected BiP and GRP94. Anti-TX antibody detected caspase 4 protein.

Caspase activity. SK-N-SH cells were seeded into 96-well culture plates (1.0×10^4 cells/well). Cells were cultured under standard conditions for 12 h, and then treated with 5 μM BIX or vehicle for another 12 h. After BIX or vehicle treatment, the whole medium was replaced with fresh medium containing 0.5 μg/ml Tm and cells were incubated for additional 36 or 48 h. After incubation, caspase-3 and -7 activity was measured using a caspase-Glo 3/7 Assay kit (Promega), according to the manufacturer's instructions. Luminescent signals were measured using a luminometer (Berthold Technologies). The measurement of caspases 3 and 7 activities was conducted in three independent experiments.

Cell death assay. SK-N-SH cells were pretreated with 5 μM BIX or vehicle for 12 h, after which the whole medium was replaced with fresh medium containing 0.5 μg/ml Tm, in which cell were cultured for the indicated times. Cells were fixed with 4% paraformaldehyde for 30 min at 4°C, washed with PBS for 5 min, and then stained with 100 μM Hoechst 33258 (Wako Pure Chemical Co., Tokyo, Japan) in PBS for 20 min. A total of 500 cells were counted randomly and apoptotic cells were determined by fluorescence microscopy.

Focal cerebral ischemia model in mice. Male adult ddY mice weighing 24–34 g (Japan SLC) were used in experiments, and were housed under diurnal lighting conditions. Anesthesia was induced by 2.0% isoflurane, then maintained using 1% isoflurane in 70% N_2O and 30% O_2 using an animal general anesthesia machine (Soft Lander, Sin-ei Industry Co. Ltd, Saitama, Japan). Body temperature was maintained between 37.0 and 37.5°C with the aid of a heating pad and heating lamp. A filament occlusion of the left MCA was carried out as previously

described.[25,26] Briefly, the left MCA was occluded with an 8-0 nylon monofilament (Ethicon, Somerville, NJ, USA) coated with a mixture of silicone resin (Xantopren; Bayer Dental, Osaka, Japan). This coated filament was introduced into the internal carotid artery through the common carotid artery up to the origin of the anterior cerebral artery, so as to occlude the MCA and posterior communicating artery. At the same time, the left common carotid artery was occluded by the suture. Permanent ischemia was selected because it produced a reproducible subtotal infarction in our previous studies.[25,26] Twenty-four hours after the occlusion, the forebrain was divided into five coronal 2 mm sections using a mouse brain matrix (RBM-2000C; Activational Systems, Warren, MI, USA). Sections were then stained with 2% TTC. Images of the infarcted areas were recorded using a digital camera (Nikon, COOLPIX4500), quantitated using Image J software (http://rsb.info.nih.gov/ij/download/), and calculated as in a previous report.[26] Brain swelling was calculated according to the following formula: (infarct volume + ipsilateral undamaged volume − contralateral volume) × 100/contralateral volume (%).[25] BIX was dissolved in 10% DMSO and fresh solution was made daily. DMSO (10%) was used as a control. Physiologic parameters were recorded according to our previously described method.[25] In brief, a polyethylene catheter was inserted into the femoral artery to sample arterial blood (30 μl) and measure blood pressure. After the catheter had been inserted into the femoral artery, 2 μl of BIX at 2.5 or 10 μg/μl was intracerebroventricularly administered 30 min before the start of the ischemia, because we do not know the permeability of BIX to the blood brain barrier. Body temperature, arterial blood pressure, pO_2, pCO_2, pH, and plasma glucose were measured 15 min after the start of the ischemia. There were no significant differences in physiological parameters between the vehicle- and BIX-treated groups (data not shown). After 30 min of ischemia, vehicle- and BIX-treated mice exhibited moderate neurological deficits (such as circling, decreased resistance to lateral pushing, decreased locomotor activity, flexion of the right (contralateral to the ischemia) torso and forelimb upon lifting the animal by its tail, and abnormal posture). Animals showing no neurological deficits at 30 min after the occlusion were removed from the study on the grounds that they had not undergone successful occlusion of the MCA. We removed 2 out of 15, 1 out of 13, and 1 out of 13 mice in control, 5 μg BIX-treated, and 20 μg BIX-treated groups, respectively. The present experiments were performed in accordance with the Guidelines for Animal Experiments of Gifu Pharmaceutical University.

Neurological deficits. Mice were tested for neurological deficits at 24 h after MCA occlusion and scored as described previously[25] using the following scale: 0 = no observable neurological deficits (normal); 1 = failure to extend the right forepaw (mild); 2 = circling to the contralateral side (moderate); 3 = loss of walking or righting reflex (severe). The investigator who rated the mice was blinded as to the group to which each mouse belonged.

Immunohistochemistry. At 24 h after MCA occlusion, mice were injected with sodium pentobarbital (nembutal; 50 mg/kg, i.p.), and then perfused through the left ventricle with 4% paraformaldehyde in 0.1 M phosphate buffer (PB; pH 7.4). Brains were removed after 15 min of perfusion fixation at 4°C and immersed in the same fixative solution overnight at 4°C. They were then immersed in 25% sucrose in 0.1 M PB for 24 h, and finally frozen in powdered dry ice. Coronal sections (10 μm) were cut on a cryostat at −20°C and stored at −80°C until use. After rehydration, endogenous peroxidase activity was quenched using 1% hydrogen peroxidase in methanol. Next, brain sections were blocked with 3% BSA in PBS/0.1% Triton X-100 for 1 h, and then incubated overnight at 4°C with primary antibody in the same buffer. Sections were washed and then incubated with biotinylated secondary antibody before being incubated for 30 min at room temperature with avidin–biotin–peroxidase complex, and then developed using diaminobenzidine (DAB) peroxidase substrate. Caspase 3-stained cells were counted in the striatum. The results are expressed as positive cells per 1 mm^2.

TUNEL staining. Apoptosis was detected using the TUNEL method using an *in situ* cell death detection kit, POD (Roche, Penzberg, Germany). TUNEL signals were developed using a DAB peroxidase substrate kit (Vector Labs, Burlingame, CA, USA).

***In situ* hybridization histochemistry.** CHOP and GAPDH cDNAs were subcloned into pGEM-T Easy and pBluescript vectors, respectively. Digoxigenin-labeled cRNA probes were made by *in vitro* transcription in the presence of digoxigenin using subcloned cDNAs for these genes as templates. *In situ* hybridization using digoxigenin-labeled cRNA probes was performed as previously described.[27]

Statistical analysis. Statistical comparisons were made using a one-way ANOVA followed by a Student's *t*-test, Dunnett's test, or the Mann–Whitney *U*-test. STATVIEW version 5.0 (SAS Institute Inc., Cary, NC, USA) was used for statistical analyses. $P<0.05$ was considered to indicate statistical significance.

Acknowledgements. We thank Dr. David Ron for the PERK$^{-/-}$ MEFs and the anti-PERK antibody, Dr. Fumihiko Urano for the IRE1$^{-/-}$ MEFs and the anti-IRE1α antibody, Dr. Laurie H Glimcher for the iATF6$\alpha\beta$MEFs, and Dr. K Mori for the BiP-pGL3 reporter plasmid. We also thank Ms Mikiko Kubo for her technical assistance. This work was supported by a Grant-in-Aid for Scientific Research (17200026) from the Japan Society for the Promotion of Science and Research on Psychiatric and Neurological Diseases and Mental Health from the Japan Ministry of Health, Labor, and Welfare. This study was supported by the Program for Promotion of Fundamental Studies in Health Sciences of the National Institute of Biomedical Innovation. Funding was also provided by the Japan Society for the Promotion of Science (SK).

1. Zhang K, Kaufman RJ. The unfolded protein response: a stress signaling pathway critical for health and disease. *Neurology* 2006; **66** (Suppl 1): s102–s109.
2. Katayama T, Imaizumi K, Sato N, Miyoshi K, Kudo T, Hitomi J *et al.* Presenilin-1 mutations downregulate the signalling pathway of the unfolded-protein response. *Nat Cell Biol* 1999; **8**: 479–485.
3. Katayama T, Imaizumi K, Honda A, Yoneda T, Kudo T, Takeda M *et al.* Disturbed activation of endoplasmic reticulum stress transducers by familial Alzheimer's disease-linked presenilin 1 mutations. *J Biol Chem* 2001; **276**: 43446–43454.
4. Yasuda Y, Kudo T, Katayama T, Imaizumi K, Yatera M, Okochi M *et al.* FAD-linked presenilin-1 mutants impede translation regulation under ER stress. *Biochem Biophys Res Commun* 2002; **296**: 313–318.
5. Hitomi J, Katayama T, Eguchi Y, Kudo T, Taniguchi M, Koyama Y *et al.* Involvement of caspase-4 in endoplasmic reticulum stress-induced apoptosis and Aβ-induced cell death. *J Cell Biol* 2004; **165**: 347–356.
6. Kitada T, Asakawa S, Hattori N, Matsumine H, Yamamura Y, Minoshima S *et al.* Mutations in the Parkin gene cause autosomal recessive juvenile Parkinsonism. *Nature* 1998; **392**: 605–608.
7. Imai Y, Soda M, Inoue H, Hattori N, Mizuno Y, Takahashi R. An unfolded putative transmembrane polypeptide, which can lead to endoplasmic reticulum stress, is a substrate of Parkin. *Cell* 2001; **105**: 891–902.
8. Nishitoh H, Matsuzawa A, Tobiume K, Saegusa K, Takeda K, Hori S *et al.* ASK1 is essential for endoplasmic reticulum stress-induced neuronal cell death triggered by expanded polyglutamine repeats. *Gene Dev* 2002; **16**: 1345–1355.
9. Bence NF, Sampat RM, Kopito RR. Impairment of the ubiquitin–proteasome system by protein aggregation. *Science* 2001; **292**: 1552–1555.
10. Kumar R, Azam S, Sullivan JM, Owen C, Cavener DR, Zhang P *et al.* Brain ischemia and reperfusion activates the eukaryotic initiation factor 2alpha kinase, PERK. *J Neurochem* 2001; **77**: 1418–1421.
11. Paschen W, Aufenberg C, Hotop S, Mengesdorf T. Transient cerebral ischemia activates processing of xbp1 messenger RNA indicative of endoplasmic reticulum stress. *J Cereb Blood Flow Metab* 2003; **23**: 449–461.
12. Boyce M, Bryant KF, Jousse C, Long K, Harding HP, Scheuner D *et al.* A selective inhibitor of eIF2α dephosphorylation protects cells from ER stress. *Science* 2005; **307**: 935–939.
13. Kim AJ, Shi Y, Austin RC, Werstuck GH. Valproate protects cells from ER stress-induced lipid accumulation and apoptosis by inhibiting glycogen synthase kinase-3. *J Cell Sci* 2005; **118**: 89–99.
14. ZaiFang Y, Luo H, Weiming F, Mattson MP. The endoplasmic reticulum stress-responsive protein GRP78 protects neurons against excitotoxicity and apotosis: suppression of oxidative stress and stabilization of calcium homeostasis. *Exp Neurol* 1999; **155**: 302–314.
15. Rao RV, Peel A, Logvinova A, del Rio G, Hermel E, Yokota T *et al.* Coupling endoplasmic reticulum stress to the cell death program: role of the ER chaperone GRP78. *FEBS Lett* 2002; **514**: 122–128.
16. Reddy RK, Mao C, Baumeister P, Austin RC, Kaufman RJ, Lee AS. Endoplasmic reticulum chaperone protein GRP78 protects cells from apoptosis induced by topoisomerase inhibitors: role of ATP binding site in suppression of caspase-7 activation. *J Biol Chem* 2003; **278**: 20915–20924.
17. Gomer C, Ferrario A, Rucker N, Wong S, Lee AS. Glucose regulated protein induction and cellular resistance to oxidative stress mediated by porphyrin photosensitization. *Cancer Res* 1991; **51**: 6574–6579.
18. Li LJ, Li X, Ferrario A, Rucker N, Liu ES, Wong S *et al.* Establishment of a Chinese hamster ovary cell line that expresses grp78 antisense transcripts and suppresses A23187 induction of both GRP78 and GRP94. *J Cell Physiol* 1992; **153**: 575–582.

19. Sugawara S, Takeda K, Lee A, Dennert G. Suppression of stress protein GRP78 induction in tumor B/C10ME eliminates resistance to cell mediated cytotoxicity. *Cancer Res* 1993; **53**: 6001–6005.
20. DeGracia DJ, Montie HL. Cerebral ischemia and the unfolded protein response. *J Neurochem* 2004; **91**: 1–8.
21. Kaufman RJ. Orchestrating the unfolded protein response in health and disease. *J Clin Invest* 2002; **110**: 1389–1398.
22. Tajiri S, Oyadomari S, Yano S, Morioka M, Gotoh T, Hamada JI *et al.* Ischemia-induced neuronal cell death is mediated by the endoplasmic reticulum stress pathway involving CHOP. *Cell Death Differ* 2004; **11**: 403–415.
23. Bertolotti A, Zhang Y, Hendershot LM, Harding HP, Ron D. Dynamic interaction of BiP and ER stress transducers in the unfolded-protein. *Nat Cell Biol* 2000; **2**: 326–332.
24. Chen D, Padiernos E, Ding F, Lossos IS, Lopez CD. Apoptosis-stimulating protein of p53-2 ($ASPP2^{53BP2L}$) is an E2F target gene. *Cell Death Differ* 2005; **12**: 358–368.
25. Hara H, Huang PL, Panahian N, Fishman MC, Moskowitz MA. Reduced brain edema and infarction volume in mice lacking the neuronal isoform of nitric oxide synthase after transient MCA occlusion. *J Cereb Blood Flow Metab* 1996; **16**: 605–611.
26. Hara H, Friedlander RM, Gagliardini V, Ayata C, Fink K, Huang Z *et al.* Inhibition of interleukin 1β converting enzyme family proteases reduces ischemic and excitotoxic neuronal damage. *Proc Natl Acad Sci USA* 1997; **94**: 2007–2012.
27. Honma Y, Kanazawa K, Mori T, Tanno Y, Tojo M, Kiyosawa H *et al.* Identification of a novel gene, OASIS, which encodes for a putative CREB/ATF family transcription factor in the long-term cultured astrocytes and gliotic tissue. *Brain Res Mol Brain Res* 1999; **69**: 93–103.

European Journal of Pharmacology 592 (2008) 138–145

Contents lists available at ScienceDirect

European Journal of Pharmacology

journal homepage: www.elsevier.com/locate/ejphar

A protective role of unfolded protein response in mouse ischemic acute kidney injury

Worapat Prachasilchai [a,1], Hiroko Sonoda [a,1], Naoko Yokota-Ikeda [b], Sayaka Oshikawa [a], Chie Aikawa [a], Kazuyuki Uchida [c], Katsuaki Ito [a], Takashi Kudo [d], Kazunori Imaizumi [e], Masahiro Ikeda [a,*]

[a] Department of Veterinary Pharmacology, Faculty of Agriculture, University of Miyazaki, Miyazaki, Japan
[b] Nephrology Division, Miyazaki Prefectural Miyazaki Hospital, Miyazaki, Japan
[c] Department of Veterinary Pathology, Faculty of Agriculture, University of Miyazaki, Miyazaki, Japan
[d] Psychiatry, Department of Integrated Medicine, Division of Internal Medicine, Osaka University Graduate School of Medicine, Suita, Japan
[e] Division of Molecular and Cellular Biology, Department of Anatomy, Faculty of Medicine, University of Miyazaki, Miyazaki, Japan

ARTICLE INFO

Article history:
Received 6 March 2008
Received in revised form 3 June 2008
Accepted 27 June 2008
Available online 5 July 2008

Keywords:
Ischemia-reperfusion injury
Endoplasmic reticulum stress
Unfolded protein response
Glucose-regulated protein 78
X-box binding protein
Tunicamycin
Thapsigargin

ABSTRACT

Although renal ischemia-reperfusion is known to activate the unfolded protein response, the renal site and role of activation of this response following the insult *in vivo* remains largely unknown. Here we studied the renal spatio-temporal expression pattern of glucose-regulated protein (GRP) 78, a central regulator of the unfolded protein response network, following renal ischemia-reperfusion and the effects of the specific chemical unfolded protein response inducers, tunicamycin and thapsigargin, on renal ischemia-reperfusion injury in mice. Renal ischemia-reperfusion resulted in expression of the spliced form of the X-box binding protein-1 (XBP-1s) transcript, an unfolded protein response target, at 1 and 2 h after the insult. This response was followed by an increase in the GRP78 transcript and protein. The increased amount of GRP78 protein after ischemia-reperfusion was largely localized in proximal tubule cells. Pretreatment with tunicamycin or thapsigargin significantly ameliorated renal dysfunction and injury after ischemia-reperfusion. Taken together with these results, the unfolded protein response was activated following renal ischemia-reperfusion at sites that are susceptible to ischemia-reperfusion injury, and this activation had a protective effect against renal ischemia-reperfusion injury *in vivo*. Molecules involved in the unfolded protein response may offer new opportunities for pharmacological intervention against renal ischemia-reperfusion injury, which is an important cause of acute kidney injury.

1. Introduction

Ischemia is an important endoplasmic reticulum stress. When protein folding in the endoplasmic reticulum is inhibited by hypoxia, multiple signal transduction pathways that allow cells to respond to hypoxic stress are triggered (Schröder and Kaufman, 2005; Feldman et al., 2005; Xu et al., 2005). These pathways are called the unfolded protein response. The 78-kDa glucose-regulated protein GRP78, also referred to as the immunoglobulin binding protein BiP, belongs to the heat shock protein 70 (HSP70) family (Benjamin and McMillan, 1998) and is a stress-inducible endoplasmic reticulum chaperone that serves as a master modulator for the unfolded protein response network. GRP78 can bind to and inhibit the activation of endoplasmic reticulum stress sensor proteins such as PKR-like endoplasmic reticulum localized kinase (PERK), inositol requiring transmembrane kinase and endonuclease (IRE) 1, and activating transcription factor (ATF) 6. When unfolded proteins accumulate, GRP78 dissociates from the endoplasmic reticulum stress sensor proteins and the unfolded protein response is launched via their activation. PERK is a serine/threonine protein kinase that phosphorylates eukaryotic initiation factor-2α (eIF2α). Phosphorylation of eIF2α inhibits protein translation. IRE1 is an endoribonuclease and kinase, and can excise an intron from the mRNA of X-box binding protein (XBP)-1. The translated protein (XBP-1s) is a basic region/leucine zipper (bZIP) transcription factor that binds to its target sequence in the regulatory regions of chaperone genes to induce their transcription. ATF6, like XBP-1s, is a bZIP transcription factor. After the active form of ATF-6 is produced in response to endoplasmic reticulum stress, it acts as a transcription factor for a range of target genes including endoplasmic reticulum chaperone genes.

Acute kidney injury is a common clinical syndrome characterized by a rapid reduction of the glomerular filtration rate (Lameire et al., 2005; Devarajan, 2006; Xue et al., 2006). Acute kidney injury has been reported in approximately 5% of hospitalized admissions and 30–50% of admissions to intensive care units. The high mortality and morbidity associated with acute kidney injury are related to a lack

* Corresponding author. Department of Veterinary Pharmacology, Faculty of Agriculture, University of Miyazaki, Gakuenkibanadai-nishi 1-1, Miyazaki 889-2192, Japan. Tel./fax: +81 985 58 7268.
E-mail address: a0d302u@cc.miyazaki-u.ac.jp (M. Ikeda).
[1] These authors contributed equally to this work.

0014-2999/$ – see front matter © 2008 Elsevier B.V. All rights reserved.
doi:10.1016/j.ejphar.2008.06.108

of understanding of its underlying molecular mechanisms, and in turn this hampers the development of specific pharmacological interventions (Lameire et al., 2005; Devarajan, 2006; Xue et al., 2006; Ikeda et al., 2006b).

Renal ischemia-reperfusion injury is an important cause of acute kidney injury. As mentioned earlier, the unfolded protein response is activated after hypoxia and therefore the unfolded protein response is thought to have an important role in the pathobiology of ischemia-reperfusion injury. Several studies have indicated that the unfolded protein response is activated after renal ischemia-reperfusion (Kuznetsov et al., 1996; Bando et al., 2004; Montie et al., 2005). However, although GRP78 is known to be a master protein for the unfolded protein response network, the localization and time course of its expression after renal ischemia-reperfusion have not been fully established.

Several specific unfolded protein response inducers, including tunicamycin, thapsigargin, and A23187, have been used in experimental studies of the unfolded protein response (Price and Calderwood, 1992; Kaufman, 1999). Studies of unfolded protein response activation in cultured renal epithelial cells have indicated that it reduces the severity of ischemia-reperfusion-induced cell injury (Bush et al., 1999; George et al., 2004). On the other hand, several *in vivo* studies have shown that treatment with tunicamycin causes apoptosis in renal tubule cells (Zinszner et al., 1998; Nakagawa et al., 2000; Marciniak et al., 2004; Takano et al., 2007). Therefore, the role of unfolded protein response activation in the pathobiology of ischemia-reperfusion injury *in vivo* remains obscure.

In order to obtain insight into the molecular mechanisms underlying renal ischemia-reperfusion injury, and to identify potential therapeutic targets against acute kidney injury, this study investigated the spatio-temporal expression pattern of GRP 78 and the effect of specific chemical unfolded protein response inducers, including tunicamycin and thapsigargin, in a mouse model of renal ischemia-reperfusion injury.

2. Materials and methods

2.1. Animals

All animal studies were in accordance with *Guide for the Care and Use of Laboratory Animals in the University of Miyazaki* and were conducted in compliance with the *Law Concerning the Protection and Control of Animals* (Japanese Law No. 105, October 1, 1973, revised on June 22, 2005), *Standards Relating to the Care and Management of Laboratory Animals and Relief of Pain*, (Notification No.88 of the Ministry of the Environment, Japan, April 28, 2006) and *Guidelines for Animal Experimentation*, (Japanese Association for Laboratory Animal Science, May 22, 1987). Male ddy mice (7 weeks old) were purchased from Kyudo, Inc. (Kumamoto, Japan). The animals were allowed free access to food and water during the study period.

2.2. Renal ischemia-reperfusion and drug administration

The renal ischemia-reperfusion procedure was performed as previously described (Yokota et al., 2002). Briefly, mice weighing 25 to 35 g were anesthetized with pentobarbital (65 to 75 mg/kg) and underwent abdominal incision and dissection of the bilateral renal pedicles. A microvascular clamp (Roboz, MD) was placed on each renal pedicle for 35 min. After the ischemic period, the clamps were removed, the wound was sutured, and the animals were allowed to recover. The animals were kept at constant body temperature with continuous monitoring during the ischemia-reperfusion period, and warmed physiological saline was given just after clamping and before suturing in order to maintain body fluid volume. The total number of animals used for evaluating the time course of renal function (Fig. 1) was 93 (sham, 48; ischemia-reperfusion, 45).

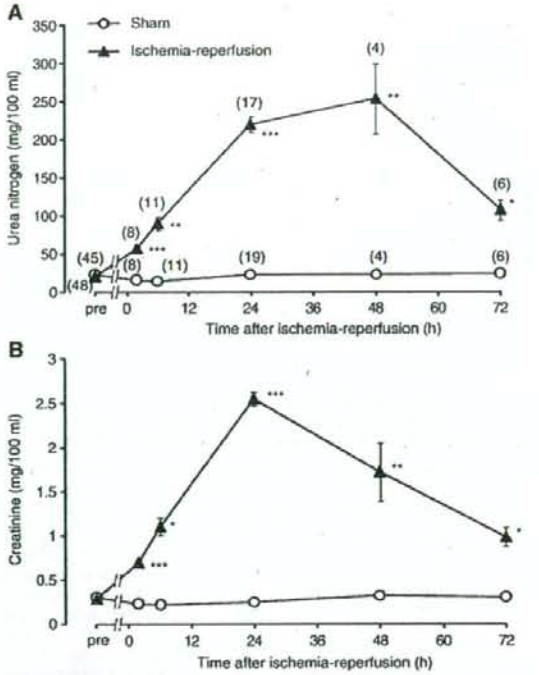

Fig. 1. Renal function after renal ischemia reperfusion. (A, B) Plasma urea nitrogen and creatinine concentrations are shown. Blood was collected more than 48 h before (pre) and 2 h, 6 h, 24 h, 48 h, and 72 h after sham (open circles) or ischemia-reperfusion (closed triangles) operation. Numbers in parentheses are the numbers of animals tested. *$P<0.05$, **$P<0.01$, and ***$P<0.001$; significantly different from the value of sham.

Tunicamycin and thapsigargin were purchased from Calbiochem (Darmstadt). Tunicamycin was dissolved in physiological saline and thapsigargin was dissolved in 100% DMSO. Tunicamycin was intraperitoneally administered to mice in a volume of 100 μL/animal 2 days prior to ischemia-reperfusion at a dosage of 1.5 mg/kg. Thapsigarin (1 mg/kg) was administered intraperitoneally to mice in a volume of 100 μL/animal at 24 h prior to ischemia-reperfusion. The control mice were given the corresponding vehicle in the same manner. The above regimen of tunicamycin and thapsigargin administration has been shown to effectively induce the unfolded protein response (Zinszner et al., 1998; Kondoh et al., 2004).

2.3. Renal function evaluation

For chemical analyses, 50-μL blood samples were obtained from the tail blood vessel using a hematocrit capillary, or 1-ml samples were obtained from the inferior vena cava under ether anesthesia at the termination point. Plasma urea nitrogen and creatinine levels were measured with an autoanalyzer (FUJIDRICHEM: Fuji Film Medical Co., Ltd. Tokyo, Japan; TBA-200FR: Toshiba Medical Systems Co., Ltd.,Tokyo, Japan).

2.4. RT-PCR analysis

Total RNA was extracted from whole kidney with the RNeasy® Protect Minikit (Qiagen) with DNase digestion and then cDNA was synthesized from 5 μg of the RNA with the iScript™ cDNA Synthesis kit® (Bio-Rad, CA), according to the respective manufacturer's instructions. Mouse XBP-1, GRP78, and GAPDH mRNA were amplified

with the following primers: forward (5′-gaaccaggagttaagaacacg-3′) and reverse (5′-aggcaacagtgtcagagtcc-3′) for XBP-1, forward (5′-cacgtccaaccccgagaa-3′) and reverse (5′-atgacccgctgatcaaagtc-3′) for GRP78, forward (5′-aacgacccccttcattgac-3′) and reverse (5′-tccacgacatactcagcac-3′) for GAPDH. The number of PCR cycles was 19 for GAPDH, 22 for GRP78, and 35 for XBP-1. All RT-PCR products were analyzed by 1.5% (GRP78 and GAPDH) or 2.5% (XBP-1) agarose gel electrophoresis.

2.5. Preparation of kidney extracts

Mouse kidneys were homogenized in ice-cold homogenate solution containing 300 mM sucrose, 25 mM imidazole, 1.3 mM EDTA, and Complete® protease inhibitor mixture (Roche Molecular Biochemicals, Germany) and the homogenates were then centrifuged at 1000 g for 10 min. The pellet was homogenized again and centrifuged at 1000 g for 10 min. The supernatants from the two centrifugations were combined and the combined solution was subsequently centrifuged at 200,000 g. The pellet from ultracentrifugation was mixed with two volumes of homogenate solution and the protein concentration in a portion of the solution was determined by a DC protein assay kit (Nippon Bio-Rad, Japan). The remaining solution was mixed with 4× Laemmli sample buffer (0.5 M Tris, pH 6.8, 50% glycerol, 8% SDS, 0.05% bromophenolblue) supplemented with 0.2 M dithiothreitol (DTT) and then incubated at 37 °C for 60 min.

2.6. Western blot analysis and chemicals

Western blot analysis was performed as previously reported (Ikeda et al., 2006a). Briefly, after separation by SDS-PAGE, the protein was transferred on to a polyvinylidene difluoride membrane and analyzed by immunoblotting. Antibody-associated protein on the membrane was detected by Super Signal® chemiluminescence detection system (Pierce, IL). Antibodies used in this study were as follows: anti-GRP78 and anti-GAPDH antibodies from Santa Cruz Biotechnology, Inc. (CA), anti-HSP70 antibody from BD Biosciences (CA).

2.7. Histopathological evaluation

For the histopathological evaluation, the left kidney was removed at the indicated time points and fixed in 10% (v/v) neutral buffered formalin. Serial sections of 2 μm thickness were stained with periodic acid-Schiff (PAS). Semi-quantitative analysis was performed by measuring the PAS-positive area. Eight microscope fields were scanned in each mouse by using an image-processing system (Nikon, Tokyo, Japan). For immunohistochemistry, the section was

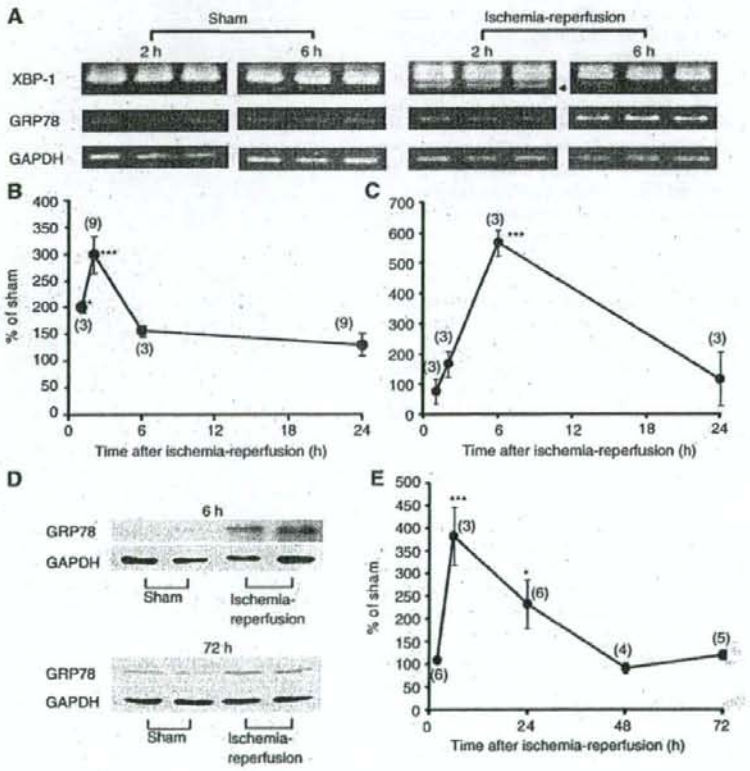

Fig. 2. XBP-1 mRNA, GRP78 mRNA, and GRP78 protein levels after renal ischemia-reperfusion. Mice were subjected to sham or ischemia-reperfusion operation and then total RNA and protein were extracted from whole kidney. (A) A splicing form of XBP-1 mRNA (arrow head) and GRP78 mRNA were determined by RT-PCR with appropriate cycle numbers. GAPDH mRNA was also examined as an internal control. (B, C) Data from the RT-PCR experiments are quantified and summarized for XBP-1s (B) and GRP78 (C) mRNA. Data are expressed as % of the mean value obtained from sham-operated mice, and values represent means ± S. E. M. Numbers in parentheses are the numbers of animals tested. (D) GRP78 and GAPDH (internal control) protein was detected by Western blot. (E) Summarized data from the Western blot experiments. Data are expressed as % of the mean value obtained from sham-operated mice, and values represent means ± S. E. M. Numbers in parentheses are the numbers of animals tested. *$P<0.05$, **$P<0.01$, and ***$P<0.001$; significantly different from the value of sham.